Saas-Fee Advanced Course 46
Swiss Society for Astrophysics and Astronomy

Mark Dijkstra
J. Xavier Prochaska
Masami Ouchi
Matthew Hayes

Lyman-alpha as an Astrophysical and Cosmological Tool

Saas-Fee Advanced Course 46. Swiss Society for Astrophysics and Astronomy

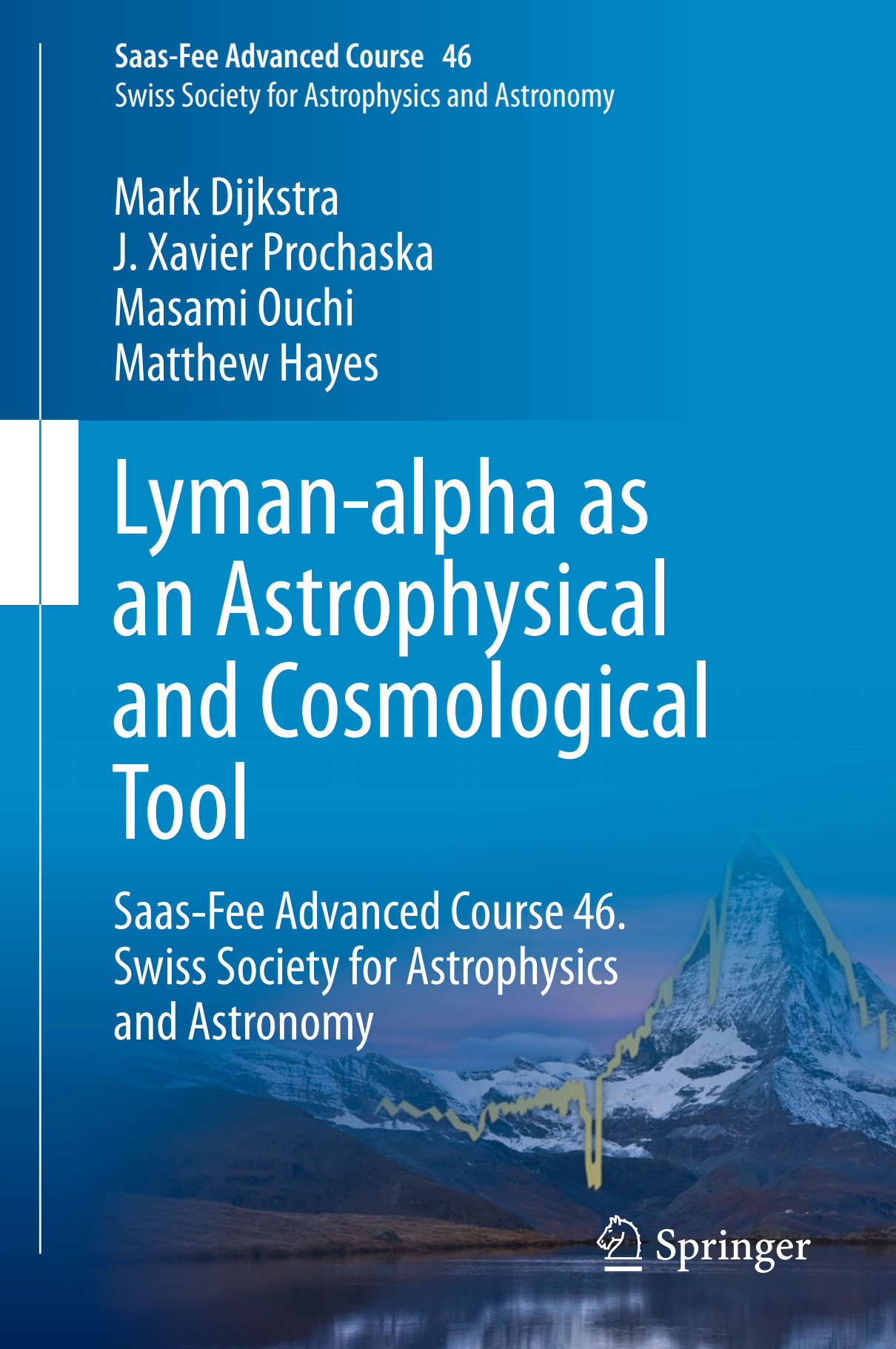

Springer

Saas-Fee Advanced Course 46

Series Editor

Swiss Society for Astrophysics and Astronomy, Sauverny, Switzerland

The Saas-Fee Advanced Courses, organized by the Swiss Society for Astrophysics and Astronomy (SSAA), have been held annually since 1971. The courses cover important and timely fields of Astrophysics and Astronomy including related fields like computational methods. They are given by two to four reputable researchers in those fields. Each lecturer covers a different aspect of the field on which he has his own expertise.

The books in this series publish the updated lecture notes of the Saas-Fee Advanced Courses. Many of them have become standard texts in their field. They are not only appreciated by graduate students, but are also used and cited as reference by researchers.

More information about this series at http://www.springer.com/series/4284

Mark Dijkstra · J. Xavier Prochaska ·
Masami Ouchi · Matthew Hayes

Lyman-alpha as an Astrophysical and Cosmological Tool

Saas-Fee Advanced Course 46

Swiss Society for Astrophysics and Astronomy
Edited by Anne Verhamme, Pierre North,
Sebastiano Cantalupo and Hakim Atek

Springer

Authors
Mark Dijkstra
Institute of Theoretical Astrophysics
University of Oslo
Oslo, Norway

J. Xavier Prochaska
Lick Observatory
University of California Observatories (UCO)
Santa Cruz, CA, USA

Masami Ouchi
Institute for Cosmic Ray Research (ICRR)
University of Tokyo
Kashiwa, Japan

Matthew Hayes
Department of Astronomy
University of Stockholm
Stockholm, Sweden

Volume Editors
Anne Verhamme
Department of Astronomy
Geneva University
Versoix, Geneva, Switzerland

Pierre North
Laboratory of Astrophysics (LASTRO)
Ecole Polytechnique Fédérale de Lausanne (EPFL)
Versoix, Geneva, Switzerland

Sebastiano Cantalupo
Institute for Astronomy
ETH Zürich
Zürich, Switzerland

Hakim Atek
Institut d'Astrophysique de Paris (IAP)
Paris, France

This Series is edited on behalf of the Swiss Society for Astrophysics and Astronomy: Société Suisse d'Astrophysique et d'Astronomie, Observatoire de Genève, ch. des Maillettes 51, CH-1290 Sauverny, Switzerland.

ISSN 1861-7980 ISSN 1861-8227 (electronic)
Saas-Fee Advanced Course
ISBN 978-3-662-59622-7 ISBN 978-3-662-59623-4 (eBook)
https://doi.org/10.1007/978-3-662-59623-4

Cover illustration: Lyman-alpha line overlaid on a photo of Matterhorn. Credit: [Vincent Favre (http://www.cristaldegivre.com) & Myriam Burgener]

This Springer imprint is published by the registered company Springer-Verlag GmbH, DE part of Springer Nature.
The registered company address is: Heidelberger Platz 3, 14197 Berlin, Germany

Preface

Hydrogen is the most abundant element in the universe, as first understood by Cecilia Payne-Gaposchkin in 1924. The Lyman α line is the strongest line of this element, making it especially important in many astrophysical topics and particularly in cosmology. Because this line falls in the ultraviolet, it has long remained unused for observational reasons, until astronomical satellites opened the UV window and until galaxies were discovered at high enough redshift to make it accessible to ground-based telescopes.

Since then, the hydrogen Lyα line has acquired ever increasing popularity to probe the deep universe, through the use of either its absorption or its emission. The Lyα forest seen in the spectra of high redshift quasars reveals the presence and distribution of absorbing gas in galaxies that would otherwise go unnoticed, and star forming galaxies can be seen to the edge of the observable universe thanks to the intensity of this line in emission. Spectroscopic confirmation of the highest redshifts known to date is generally based on the Lyα line. However, the very visibility of this resonance line when seen in emission is linked with its extremely high opacity, so that the interpretation of the Lyα profile is far from straightforward. Careful modeling is needed to understand the observations, because transfer effects are important enough to prevent, for instance, any simple translation of the line position and width in terms of mean radial velocity and velocity dispersion.

The 46th Saas-Fee advanced course of the Swiss Society for Astrophysics and Astronomy, entitled *Lyman-α as an astrophysical and cosmological tool*, took place in Les Diablerets, a mountain resort of the Swiss Alps. Exceptionally, as many as four lecturers (instead of three according to tradition) have contributed to this successful course: Mark Dijkstra, J. Xavier Prochaska, Masami Ouchi, and Matthew Hayes. The four contributions to this book review respectively the theoretical aspects of the Lyα line formation, and three aspects of how this line is used in extragalactic astronomy: absorption of intervening hydrogen clouds in the line of sight of quasars, Lyα emitting galaxies at high redshift, and detailed emission and absorption processes in local galaxies. Such topics cover much of today's endeavours in observational cosmology, so this book should prove useful and timely for many Ph.D. students as well as more advanced researchers. We are aware of an extragalactic bias, in the

sense that this book does not adress more local applications of the Lyα line, such as the study of exoplanet atmospheres. Even so, students in the latter field may still find interest in at least Mark Dijkstra's theoretical contribution.

We thank Mrs. Myriam Burgener, the Secretary of the Département d'Astronomie de l'Université de Genève, for her very efficient help in the organization of the course and for her presence during the whole event. This course, attended by 65 participants from many countries, was sponsored by the Swiss Society for Astrophysics and Astronomy, the Swiss Academy of Sciences, the Ecole Polytechnique Fédérale de Lausanne (EPFL), and the University of Geneva.

Versoix, Switzerland
March 2018

Anne Verhamme
Pierre North
Hakim Atek
Sebastiano Cantalupo

Contents

Contributors

Mark Dijkstra Institute of Theoretical Astrophysics, University of Oslo, Oslo, Norway, e-mail: astromark77@gmail.com

Matthew Hayes Department of Astronomy & OKC, AlbaNova University Centre, University of Stockholm, Stockholm, Sweden, e-mail: matthew@astro.su.se

Masami Ouchi Institute for Cosmic Ray Research (ICRR), University of Tokyo, Kashiwa, Japan, e-mail: ouchims@icrr.u-tokyo.ac.jp

J. Xavier Prochaska Lick Observatory, University of California Observatories (UCO), Santa Cruz, CA, USA, e-mail: xavier@ucolick.org

Chapter 1
Physics of Lyα Radiative Transfer

Mark Dijkstra

1.1 Introduction

Half a century ago, [205] predicted that the Lyα line should be a good tracer of star forming galaxies at large cosmological distances. This statement was based on the assumption that ionizing photons that are emitted by young, newly formed stars are efficiently reprocessed into recombination lines, of which Lyα contains the largest flux. In the past two decades the Lyα line has indeed proven to provide us with a way to both find and identify galaxies out to the highest redshifts (currently as high as $z = 8.7$, see [290]). In addition, we do not only expect Lyα emission from (star forming) galaxies, but from structure formation in general (e.g. [94]). Galaxies are surrounded by vast reservoirs of gas that are capable of both emitting and absorbing Lyα radiation. Observed spatially extended Lyα nebulae (or 'blobs') may indeed provide insight into the formation and evolution of galaxies, in ways that complement direct observations of galaxies.

The original version of this chapter was revised: Figure 1.35 has been updated and in Page "52" an equation has been corrected. The correction to this chapter can be found at https://doi.org/10.1007/978-3-662-59623-4_5

M. Dijkstra (✉)
University of Oslo, Oslo, Norway
e-mail: astromark77@gmail.com

M. Dijkstra et al., *Lyman-alpha as an Astrophysical and Cosmological Tool*,
Saas-Fee Advanced Course 46, https://doi.org/10.1007/978-3-662-59623-4_1

Many new instruments and telescopes[1] are either about to be, or have just been, commissioned that are ideal for targeting the redshifted Lyα line. The sheer number of observed Lyα emitting sources is expected to increase by more than two orders of magnitude at all redshifts $z \sim 2$–7. For comparison, this boost is similar to that in the number of known exoplanets as a result of the launch of the Kepler satellite. In addition, sensitive integral field unit spectrographs will allow us to (*i*) detect sources that are more than an order of magnitude fainter than what has been possible so far, (*ii*) take spectra of faint sources, (*iii*) take spatially resolved spectra of the more extended sources, and (*iv*) detect phenomena at surface brightness levels at which diffuse Lyα emission from the environment of galaxies is visible.

In order to interpret this growing body of data, we must understand the radiative transfer of Lyα photons from its emission site to the telescope. Lyα transfer depends sensitively on the gas distribution and kinematics. This complicates interpretation of Lyα observations. On the other hand, the close interaction of the Lyα radiation field and gaseous flows in and around galaxies implies that observations of Lyα contains information on the medium through which the photons were scattering, and may thus present an opportunity to learn more about atomic hydrogen in gaseous flows in and around galaxies.

1.2 The Hydrogen Atom and Introduction to Lyα Emission Mechanisms

1.2.1 Hydrogen in Our Universe

It has been known from almost a century that hydrogen is the most abundant element in our Universe. In 1925 Cecilia Payne demonstrated in her PhD dissertation that the Sun was composed primarily of hydrogen and helium. While this conclusion was controversial[2] at the time, it is currently well established that hydrogen accounts for the majority of baryonic mass in our Universe: the fluctuations in the Microwave Background as measured by the Planck satellite [211] imply that baryons account for 4.6% of the Universal energy density, and that hydrogen accounts for 76% of the

[1] Examples of new instruments/telescopes that will revolutionize our ability to target the Lyα emission line: the Hobby-Eberly Telescope Dark Energy Experiment (HETDEX, http://hetdex.org/) will increase the sample of Lyα emitting galaxies by orders of magnitude at $z \sim 2$–4; Subaru's Hyper Suprime-Cam (http://www.naoj.org/Projects/HSC/) is expected to provide a similar boost out to $z \sim 7$. Integral Field Unit Spectrographs such as MUSE (https://www.eso.org/sci/facilities/develop/instruments/muse.html, also see the Keck Cosmic Web Imager http://www.srl.caltech.edu/sal/keck-cosmic-web-imager.html) will allow us to map out spatially extended Lyα emission down to $\sim$10 times lower surface brightness levels, and take spatially resolved spectra. In the (near) future, telescopes such as the James Webb Space Telescope (JWST, http://www.jwst.nasa.gov/) and ground based facilities such as the Giant Magellan Telescope (http://www.gmto.org/) and ESO's E-ELT (http://www.eso.org/public/usa/teles-instr/e-elt/, http://www.tmt.org/ (TMT).

[2] See https://en.wikipedia.org/wiki/Cecilia_Payne-Gaposchkin.

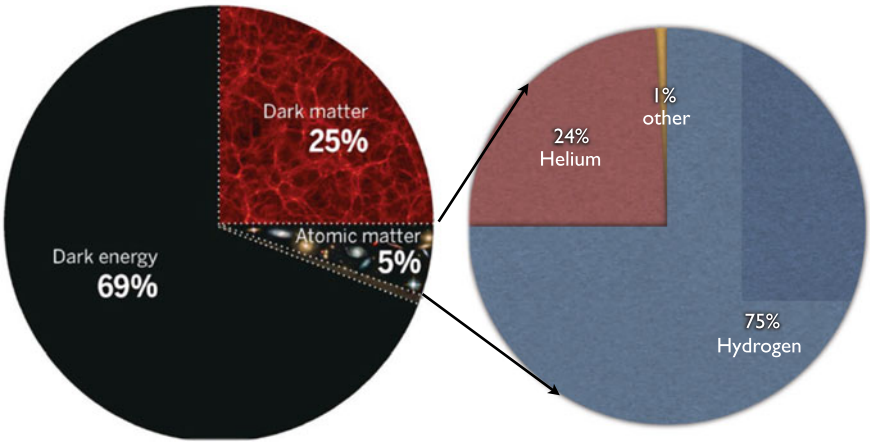

Fig. 1.1 Relative contributions to Universal energy/mass density. Most (∼70%) of the Universal energy content is in the form of dark energy, which is an unknown hypothesized form of energy which permeates all of space, and which is responsible for the inferred acceleration of the expansion of the Universe. In addition to this, ∼25% is in the form of dark matter, which is a pressureless fluid which acts only gravitationally with ordinary matter. Only ∼5% of the Universal energy content is in the form of ordinary matter like baryons, leptons etc. Of this component, ∼75% of all baryonic matter is in Hydrogen, while the remaining 25% is almost entirely Helium. Observing lines associated with atomic hydrogen is therefore an obvious way to go about studying the Universe

total baryonic mass. The remaining 24% is in the form of helium (see Fig. 1.1). The leading constraints on these mass ratios come from Big Bang Nucleosynthesis, which predicts a hydrogen abundance of ∼75% by mass for the inferred Universal baryon density ($\Omega_b h^2 = 0.022$, [211]). Additional constraints come from observations of hydrogen and emission lines of extragalactic, metal poor HII regions [15, 134].

Because of its prevalence throughout the Universe, lines associated with atomic hydrogen have provided us with a powerful window on our Universe. The 21-cm hyperfine transition was observed from our own Milky Way by Ewen and Purcell in [81], shortly after it was predicted to exist by Jan Oort in 1944. Observations of the 21-cm line have allowed us to perform precise measurements of the distribution and kinematics of neutral gas in external galaxies, which provided evidence for dark matter on galactic scales (e.g. [33]). Detecting the redshifted 21-cm emission from galaxies at $z > 0.5$, and from atomic hydrogen in the diffuse (neutral) intergalactic medium represent the main science drivers for many low frequency radio arrays that are currently being developed, including the Murchinson Wide Field Array,[3] the Low Frequency Array,[4] The Hydrogen Epoch of Reionization Array (HERA),[5] the

[3] http://www.mwatelescope.org/.
[4] http://www.lofar.org/.
[5] http://reionization.org/.

Precision Array for Probing the Epoch of Reionization (PAPER),[6] and the Square Kilometer Array.[7]

Similarly, the Lyα transition has also revolutionized observational cosmology: observations of the Lyα forest in quasar spectra has allowed us to measure the matter distribution throughout the Universe with unprecedented accuracy. The Lyα forest still provides an extremely useful probe of cosmology on scales that are not accessible with galaxy surveys, and/or the Cosmic microwave background. The Lyα forest will be covered extensively in the lectures by J. X. Prochaska. So far, the most important contributions to our understanding of the Universe from Lyα have come from studies of Lyα absorption. However, with the commissioning of many new instruments and telescopes, there is tremendous potential for Lyα in emission. Because Lyα is a resonance line, and because typical astrophysical environments are optically thick to Lyα, we need to understand the radiative transfer to be able to fully exploit the observations of Lyα emitting sources.

1.2.2 The Hydrogen Atom: The Classical and Quantum Picture

The classical picture of the hydrogen atom is that of an electron orbiting a proton. In this picture, the electrostatic force binds the electron and proton. The equation of motion for the electron is given by

$$\frac{q^2}{r^2} = \frac{m_e v_e^2}{r}, \tag{1.1}$$

where q denotes the charge of the electron and proton, and the subscript 'e' ('p') indicates quantities related to the electron (proton). The acceleration the electron undergoes thus equals $a_{\rm e} = \frac{v_e^2}{r} = \frac{q^2}{r^2 m_e}$. When a charged particle accelerates, it radiates away its energy in the form of electromagnetic waves. The total energy that is radiated away by the electron per unit time is given by the Larmor formula, which is given by

$$P = \frac{2}{3}\frac{q^2 a_e^2}{c^3}. \tag{1.2}$$

The total energy of the electron is given by the sum of its kinetic and potential energy, and equals $E_e = \frac{1}{2} m_e v_e^2 - \frac{q^2}{r} = -\frac{q^2}{2r}$. The total time it takes for the electron to radiative away all of its energy is thus given by

$$t = \frac{E_e}{P} = \frac{3c^3}{4 r a_e^2} = \frac{3 r^3 m_e^2 c^3}{4 q^4} \approx 10^{-11}\ {\rm s}, \tag{1.3}$$

[6] http://eor.berkeley.edu/.

[7] https://www.skatelescope.org/.

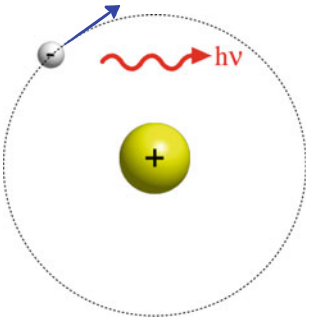

Fig. 1.2 In the classical picture of the hydrogen atom, an electron orbits a central proton at $v \sim \alpha c$. The acceleration that the electron experiences causes it to emit electromagnetic waves and loose energy. This causes the electron to spiral inwards into the proton on a time-scale of $\sim 10^{-11}$ s. In the classical picture, hydrogen atoms are highly unstable, short-lived objects

where we substituted the Bohr radius for r, i.e. $r = a_0 = 5.3 \times 10^{-9}$cm. In the classical picture, hydrogen atoms would be highly unstable objects, which is clearly problematic and led to the development of quantum mechanics (Fig. 1.2).

In quantum mechanics, electron orbits are *quantized*: In Niels Bohr's model of the atom, electrons can only reside in discrete orbitals. While in such an orbital, the electron does not radiate. It is only when an electron transitions from one orbital to another that it emits a photon. Quantitatively, the total angular momentum of the electron $L \equiv m_e v_e r$ can only taken on discrete values $L = n\hbar$, where $n = 1, 2, ...$, and $\hbar$ denotes the reduced Planck constant (Table 1.1). The total energy of the electron is then

$$E_e(n) = -\frac{q^4 m_e}{2n^2\hbar^2} = -\frac{E_0}{n^2}, \tag{1.4}$$

where $E_0 = 13.6$ eV denotes 1 Rydberg, which corresponds to the binding energy of the electron in its ground state. In quantum mechanics, the total energy of an electron bound to a proton to form a hydrogen atom can only take on a discrete set of values, set by the 'principal quantum number' n. The quantum mechanical picture of the hydrogen atom differs from the classical one in additional ways: the electron orbital of a given quantum state (an orbital characterized by quantum number n) does not correspond to the classical orbital described above. Instead, the electron is described by a quantum mechanical wavefunction $\psi(\mathbf{r})$, (the square of) which describes the probability of finding the electron at some location $\mathbf{r}$. The functional form of these wavefunctions are determined by the Schrödinger equation. We will not discuss the Schrödinger equation in these lectures, but will simply use that it implies that the quantum mechanical wavefunction $\psi(\mathbf{r})$ of the electron is characterized fully by *two* quantum numbers: the principal quantum number n, and the orbital quantum number l. The orbital quantum number l can only take on the values $l = 0, 1, 2, ..., n-1$. The electron inside the hydrogen atom is fully characterized by these two numbers. The classical analogue of requiring two numbers to characterize the electron wavefunction

Table 1.1 Symbol dictionary

Symbol	Definition
$k_{\rm B}$	Boltzmann constant: $k_B = 1.38 \times 10^{-16}$ erg K^{-1}
$h_{\rm P}$	Planck constant: $h_P = 6.67 \times 10^{-27}$ erg s
$\hbar$	Reduced Planck constant: $\hbar = \frac{h_{\rm P}}{2\pi}$
$m_{\rm p}$	Proton mass: $m_p = 1.66 \times 10^{-24}$
$m_{\rm e}$	Electron mass: $m_{\rm e} = 9.1 \times 10^{-28}$ g
q	Electron charge: $q = 4.8 \times 10^{-10}$ esu
c	Speed of light: $c = 2.9979 \times 10^{10}$ cm s^{-1}
ΔE_{ul}	Energy difference between upper level 'u' and lower level 'l' (in ergs)
ν_{ul}	Photon frequency associated with the transition $u \rightarrow l$ (in Hz)
f_{ul}	The oscillator strength associated with the transition $u \rightarrow l$ (dimensionless)
A_{ul}	Einstein A-coefficient of the transition $u \rightarrow l$ (in s^{-1})
B_{ul}	Einstein B-coefficient of the transition $u \rightarrow l$: $B_{ul} = \frac{2h_P\nu_{ul}^3}{c^2} A_{ul}$ (in erg cm^{-2} s^{-1})
B_{lu}	Einstein B-coefficient of the transition $l \rightarrow u$: $B_{lu} = \frac{g_u}{g_l} B_{ul}$
$\alpha_{A/B}$	Case A /B recombination coefficient (in cm^3 s^{-1})
α_{nl}	Recombination coefficient into state (n, l) (in cm^3 s^{-1})
$g_{u/l}$	Statistical weight of upper/lower level of a radiative transition (dimensionless)
ν_α	Photon frequency associated with the Lyα transition: $\nu_\alpha = 2.47 \times 10^{15}$ Hz
ω_α	Angular frequency associated with the Lyα transition: $\omega_\alpha = 2\pi\,\nu_\alpha$
λ_α	Wavelength associated with the Lyα transition: $\lambda_\alpha = 1215.67$ Å
A_α	Einstein A-coefficient of the Lyα transition: $A_\alpha = 6.25 \times 10^8$ s^{-1}
T	gas temperature (in K)
$\nu_{\rm th}$	Velocity dispersion (times $\sqrt{2}$): $\nu_{\rm th} = \sqrt{\frac{2k_BT}{m_p}}$
$\nu_{\rm turb}$	Turbulent velocity dispersion
b	Doppler broadening parameter : $b = \sqrt{\nu_{\rm th}^2 + \nu_{\rm turb}^2}$
$\Delta\nu_\alpha$	Doppler induced photon frequency dispersion:$\Delta\nu_\alpha = \nu_\alpha \frac{b}{c}$ (in Hz)
x	'Normalized' photon frequency: $x = (\nu - \nu_\alpha)/\Delta\nu_\alpha$ (dimensionless)
$\sigma_\alpha(x)$	Lyα Absorption cross-section at frequency x (in cm^2), $\sigma_\alpha(x) = \sigma_{\alpha,0}\phi(x)$
$\sigma_{\alpha,0}$	Lyα Absorption cross-section at line center, $\sigma_{\alpha,0} = 5.9 \times 10^{-14}\left(\frac{T}{10^4\ {\rm K}}\right)^{-1/2}$ cm^2
$\phi(x)$	Voigt profile (dimensionless)
a_ν	Voigt parameter: $a_\nu = A_\alpha/[4\pi\Delta\nu_\alpha] = 4.7 \times 10^{-4}(T/10^4\ {\rm K})^{-1/2}$
I_ν	Specific intensity (in erg s^{-1} Hz^{-1} cm^{-2} sr^{-1})
J_ν	Angle averaged specific intensity (in erg s^{-1} Hz^{-1} cm^{-2} sr^{-1})

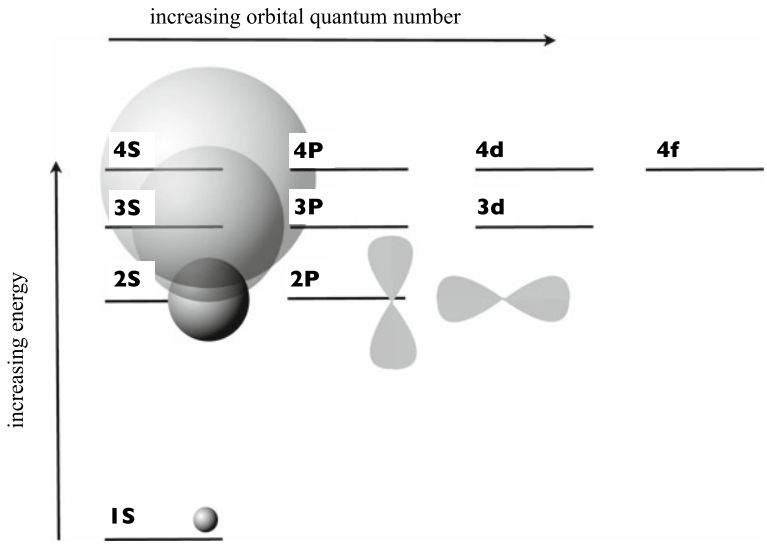

Fig. 1.3 The total energy of the quantum states of the hydrogen atom, and a simplified representation of the associated quantum mechanical wavefunction describing the electron. The level denoted with '1s' denotes the ground state and has a total energy $E = -13.6$ eV. The wavefunction is spherically symmetric and compact. The extent/size of the wavefunction increases with quantum number n. The eccentricity/elongation of the wavefunction increases with quantum number l. The orientation of non-spherical wavefunction can be represented by a third quantum number m

is that we need two numbers to characterize the classical orbit of the electron around the proton, namely energy E and total angular momentum L.

The diagram in Fig. 1.3 shows the total energy of different quantum states in the hydrogen, and a sketch of the associated wavefunctions. This Figure indicates that

- The lowest energy state corresponds to the $n = 1$ state, with an energy of $E = -13.6$ eV. For the state $n = 1$, the orbital quantum number l can only take on the value $l = 0$. This state with $(n, l) = (1, 0)$ is referred to as the '1s'-state. The '1' refers to the value of n, while the 's' is a historical way (the 'spectroscopic notation') of labelling the '$l = 0$'-state. This Figure also indicates (schematically) that the wavefunction that describes the $1s$-state is spherically symmetric. The 'size' or extent of this wavefunction relates to the classical atom size in that the expectation value of the radial position of the electron corresponds to the Bohr radius a_0, i.e. $\int dV r|\psi_{1s}(\mathbf{r})|^2 = a_0$.
- The second lowest energy state, $n = 2$, has a total energy $E = E_0/n^2 = -3.4$ eV. For this state there exist two quantum states with $l = 0$ and $l = 1$. The '2s'-state is again characterized by a spherically symmetric wavefunction, but which is more extended. This larger physical extent reflects that in this higher energy state, the electron is more likely to be further away from the proton, completely in line with classical expectations. On the other hand, the wavefunction that describes the '2p'-state ($n = 2, l = 1$) is not spherically symmetric, and consists of two 'lobes'.

The elongation that is introduced by these lobes can be interpreted as the electron being on an eccentric orbit, which reflects the increase in the electron's orbital angular momentum.

- The third lowest energy state $n = 3$ has a total energy of $E = E_0/n^2 = -1.5$ eV. The size/extent of the orbital/wavefunction increases further, and the complexity of the shape of the orbitals increases with n (see e.g. https://en.wikipedia.org/wiki/Atomic_orbital for illustrations). Loosely speaking, the quantum number n denotes the extent/size of the wavefunction, l denotes its eccentricity/elongation. The orientation of non-spherical wavefunction can be represented by a third quantum number m.

1.2.3 Radiative Transitions in the Hydrogen Atom: Lyman, Balmer, ..., Pfund, ... Series

We discussed how in the classical picture of the hydrogen atom, the electron ends up inside the proton after $\sim 10^{-11}$ s. In quantum mechanics, the electron is only stable in the ground state (1s). The life-time of an atom in any excited state is very short, analogous to the instability of the atom in the classical picture. Transitions between different quantum states have been historically grouped into series, and named after the discoverer of these series. The series include

- **The Lyman series**. A series of radiative transitions in the hydrogen atom which arise when the electron goes from $n \geq 2$ to $n = 1$. The first line in the spectrum of the Lyman series—named Lyman α (hereafter, Lyα)—was discovered in 1906 by Theodore Lyman, who was studying the ultraviolet spectrum of electrically excited hydrogen gas. The rest of the lines of the spectrum were discovered by Lyman in subsequent years.
- **The Balmer series**. The series of radiative transitions from $n \geq 3$ to $n = 2$. The series is named after Johann Balmer, who discovered an empirical formula for the wavelengths of the Balmer lines in 1885. The Balmer-α (hereafter Hα) transition is in the red, and is responsible for the reddish glow that can be seen in the famous Orion nebula.
- Following the Balmer series, we have the **Paschen series** ($n \geq 4 \rightarrow n = 3$), the **Brackett series** ($n \geq 5 \rightarrow 4$), the **Pfund series** ($n \geq 6 \rightarrow 5$), ... Especially Pfund-δ is potentially an interesting probe ([199]-2016 private communication).

Quantum mechanics does not allow radiative transitions between just any two quantum states: these radiative transitions must obey the 'selection rules'. The simplest version of the selection rules—which we will use in these lectures—is that only transitions of the form $|\Delta l| = 1$ are allowed. A simple interpretation of this is that photons carry a (spin) angular momentum given by $\hbar$, which is why the angular momentum of the electron orbital must change by $\pm\hbar$ as well. Figure 1.4 indicates allowed transitions, either as *green solid lines* or as *red dashed lines*. Note that the Lyman-β, γ, ... transitions ($3p \rightarrow 1s$, $4p \rightarrow 1s$, ...) are not shown on purpose. As

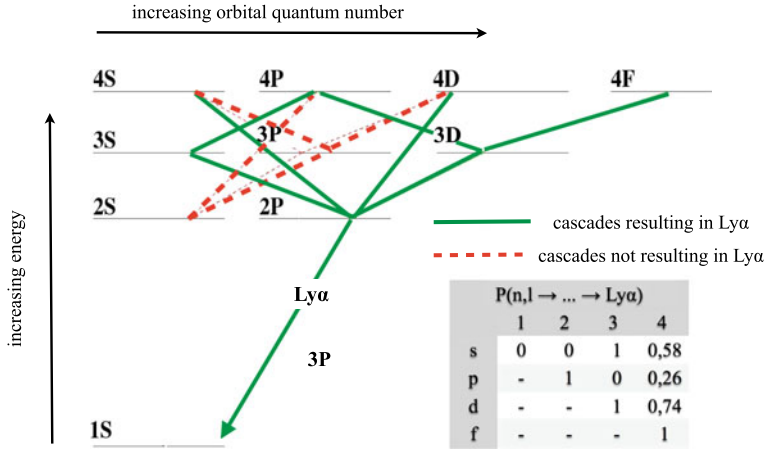

Fig. 1.4 Atoms in any state with $n > 1$ radiatively cascade back down to the ground (1s) state. The quantum mechanical selection rules only permit transitions where $|\Delta l| = 1$. These transitions are indicated with colored lines connecting the different quantum states. The *green solid lines* indicate radiative cascades that result in the emission of a Lyα photon, while *red dotted lines* indicate transitions that do not. We have omitted all direct radiative transitions $np \rightarrow 1s$: this corresponds to the 'case-B' approximation, which assumes that the recombining gas is optically thick to all Lyman-series photons, and that these photons would be re-absorbed immediately. The table in the lower right corner indicates Lyα production probabilities from various states: e.g. the probability that at atom in the $4s$ state produces a Lyα photon is ∼0.58. *Credit from Fig.* 1 *of* [75], *Lyman Alpha Emitting Galaxies as a Probe of Reionization, PASA, 31, 40D*

we will see later in the lectures, while these transitions are certainly allowed, in realistic astrophysical environments it is better to simply ignore them.

Consider an electron in some arbitrary quantum state (n, l). The electron does not spend much time in this state, and radiatively decays down to a lower energy state (n', l'). This lower energy state is again unstable [unless $(n', l') = (1, 0)$], and the electron again radiatively decays to an even lower energy state (n'', l''). Ultimately, all paths lead to the ground state, even those paths that go through the $2s$ state. While the selection rules do not permit transitions of the form $2s \rightarrow 1s$, these transitions can occur, if the atom emits *two* photons (rather than one). Because these two-photon transitions are forbidden, the life-time of the electron in the $2s$ state is many orders of magnitude larger than almost all other quantum states (it is ∼8 orders of magnitude longer than that of the $2p$-state), and this quantum state is called 'meta-stable'. The path from an arbitrary quantum state (n, l) to the ground state via a sequence of radiative decays is called a 'radiative cascade'.

The *green solid lines* in Fig. 1.4 show radiative cascades that result in the emission of a Lyα photon. The *red dashed lines* show the other radiative cascades. The table in the *lower right corner* shows the probability that a radiative cascade from quantum state (n, l) produces a Lyα photon. This probability is denoted with $P(n, l \rightarrow ... \rightarrow$ Lyα). For example, the probability that an electron in the $2s$ orbital gives rise to Lyα

is zero. The probability that an electron in the $3s$ orbital gives Lyα is 1. This is because the only allowed radiative cascade to the ground state from $3s$ is $3s \rightarrow 2p \rightarrow 1s$. This last transition corresponds to the Lyα transition. For $n \geq 4$ the probabilities become non-trivial, as we have to compute the likelihood of different radiative cascades. We discuss this in more detail in the next section.

1.2.4 Lyα Emission Mechanisms

A hydrogen atom emits Lyα once its electron is in the $2p$ state and decays to the ground state. We mentioned qualitatively how radiative cascades from a higher energy state can give rise to Lyα production. Electrons can end up these higher energy quantum states (any state with $n > 1$) in two different ways:

1. **Collisions.** The 'collision' between an electron and a hydrogen atom can leave the atom in an excited state, at the expense of kinetic energy of the free electron. This process is illustrated in Fig. 1.5. This process converts thermal energy of the electrons, and therefore of the gas as whole, into radiation. This process is also referred to as Lyα production via 'cooling' radiation. We discuss this process in more detail in Sect. 1.3.1, and in which astrophysical environments it may occur in Sect. 1.4.
2. **Recombination**. Recombination of a free proton and electron can leave the electron in any quantum state (n, l). Radiative cascades to the ground state can then produce a Lyα photon. As we discussed in Sect. 1.2.3, we can compute the probability that each quantum state (n, l) produces a Lyα photon during the radiative cascade down to the ground-state. If we sum over all these quantum states, and properly weigh by the probability that the freshly combined electron-proton pair ended up in state (n, l), then we can compute the probability that a recombination event gives us a Lyα photon. We discuss the details of this calculation in Sect. 1.3.2. Here, we simply discuss the main results.
   The *upper panel* of Fig. 1.6 shows the total probability $P(\text{Ly}\alpha)$ that a Lyα photon is emitted per recombination event as a function of gas temperature T. This plot contains two lines. The *solid black line* represents 'Case-A', which refers to the most general case where we allow the electron and proton to recombine into *any* state (n, l), and where we allow for all radiative transitions permitted by the selection rules. The *dashed black line* shows 'Case-B', which refers to the case where we do not allow for (*i*) direct recombination into the ground state, which produces an ionizing photon, and (*ii*) radiative transitions of the higher order Lyman series, i.e. Lyβ, Lyγ, Lyδ,.... Case-B represents that most astrophysical gases efficiently re-absorb higher order Lyman series and ionizing photons, which effectively 'cancels out' these transitions (see Sect. 1.3.2 for more discussion on this). This Figure shows that for gas at $T = 10^4$ K and case-B recombination, we have $P(\text{Ly}\alpha) = 0.68$. This value '0.68′ is often encountered during discussions on Lyα emitting galaxies. It is worth keeping in mind that

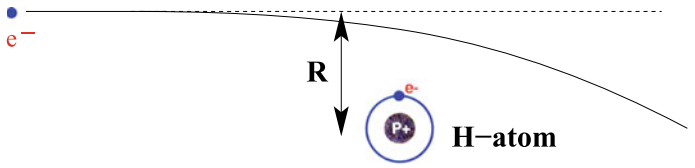

Fig. 1.5 Cooling radiation at the atomic level: an interaction between an electron and a hydrogen atom can leave the hydrogen atom in an excited state, which can produce a Lyα photon. The energy carried by the Lyα photon comes at the expense of the kinetic energy of the electron. Lyα emission by the hydrogen atom thus cools the gas

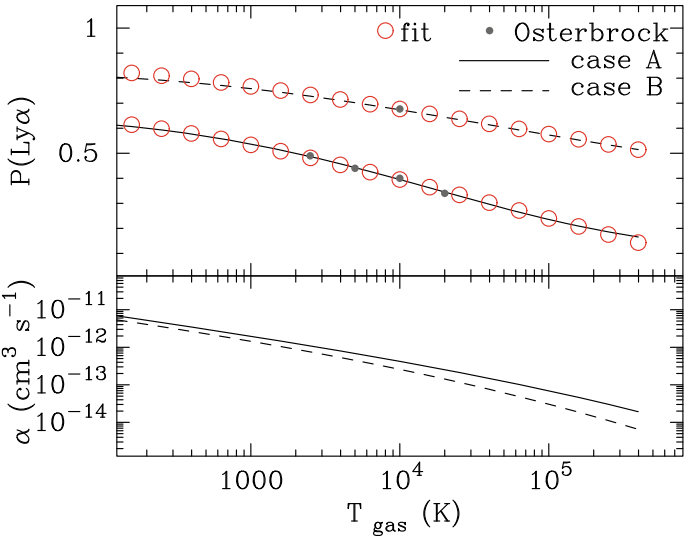

Fig. 1.6 The *top panel* shows the probability $P(\text{Ly}\alpha)$ that a recombination event leads to the production of a Lyα photon, as a function of gas temperature T. The *upper dashed line* (*lower solid line*) corresponds to 'case B' ('case A'). The *lower panel* shows the recombination rate $\alpha(T)$ (in $\text{cm}^3\ \text{s}^{-1}$) at which electrons and protons recombine. The *solid line* (*dashed line*) represents case-B (case-A). The *red open circles* represent fitting formulae (Eq. 1.5). *Credit from Fig. 2 of* [75], *Lyman Alpha Emitting Galaxies as a Probe of Reionization, PASA, 31, 40D*

the probability $P(\text{Ly}\alpha)$ increases with decreasing gas temperature and can be as high as $P(\text{Ly}\alpha) = 0.77$ for $T = 10^3$ K (also see [42]). The *red open circles* represent the following two fitting formulae

$$P_{\rm A}(\text{Ly}\alpha) = 0.41 - 0.165 \log T_4 - 0.015 (T_4)^{-0.44}$$
$$P_{\rm B}(\text{Ly}\alpha) = 0.686 - 0.106 \log T_4 - 0.009 (T_4)^{-0.44}, \qquad (1.5)$$

where $T_4 \equiv T/10^4$ K. The fitting formula for case-B is taken from [42].

1.3 A Closer Look at Lyα Emission Mechanisms and Sources

The previous section provided a brief description of physical processes that give rise to Lyα emission. Here, we discuss these in more detail, and also link them to astrophysical sources of Lyα.

1.3.1 Collisions

Collisions involve an electron and a hydrogen atom. The efficiency of this process depends on the relative velocity of the two particles. The Lyα production rate therefore includes the product of the number density of both species, and the rate coefficient $q_{1s2p}(P[v_{\rm e}])$ which quantifies the velocity dependence of this process ($P[v_{\rm e}]$ denotes the velocity distribution of electrons). If we assume that the velocity distribution of electrons is given by a Maxwellian distribution, then $P[v_{\rm e}]$ is uniquely determined by temperature T, and the rate coefficient becomes a function of temperature, $q_{1s2p}(T)$. The total Lyα production rate through collisional excitation is therefore

$$R_{\rm coll}^{\rm Ly\alpha} = n_e n_{\rm H} q_{1s2p}\ {\rm cm}^{-3}\ {\rm s}^{-1}. \tag{1.6}$$

In general, the rate coefficient q_{lu} is expressed[8] in terms of a 'velocity averaged collision strength' $\langle\Omega_{lu}\rangle$ as

$$q_{lu} = \frac{h_P^2}{(2\pi m_e)^{3/2}(k_B T)^{1/2}} \frac{\langle\Omega_{lu}\rangle}{g_l} \exp\Big(-\frac{\Delta E_{lu}}{k_B T}\Big) = 8.63\times10^{-6} T^{-1/2} \frac{\langle\Omega_{lu}\rangle}{g_l} \exp\Big(-\frac{\Delta E_{lu}}{k_B T}\Big)\ {\rm cm}^3\ {\rm s}^{-1}. \tag{1.7}$$

Calculating the collision strength is a very complex problem, because for the free-electron energies of interest, the free electron spends a relatively long time near the target atom, which causes distortions in the bound electron's wavefunctions. Complex quantum mechanical interactions may occur, and especially for collisional excitation into higher-n states, multiple scattering events become important (see [26] and references therein). The most reliable collision strengths in the literature are for the $1s \rightarrow nL$, with $n < 4$ and $L < d$ [9, 198, 236]. The *left panel* of Fig. 1.7 shows the velocity averaged collision strength for several transitions. There exist some differences in the calculations between these different groups. Collisional excitation rates still appear uncertain at the 10–20% level.

As we mentioned above, radiation is produced in collisions at the expense of the gas' thermal energy. The total rate at which the gas looses thermal energy, i.e. cools, per unit volume is

[8]The subscripts 'l' and 'u' refer to the 'lower' and 'upper' energy states, respectively.

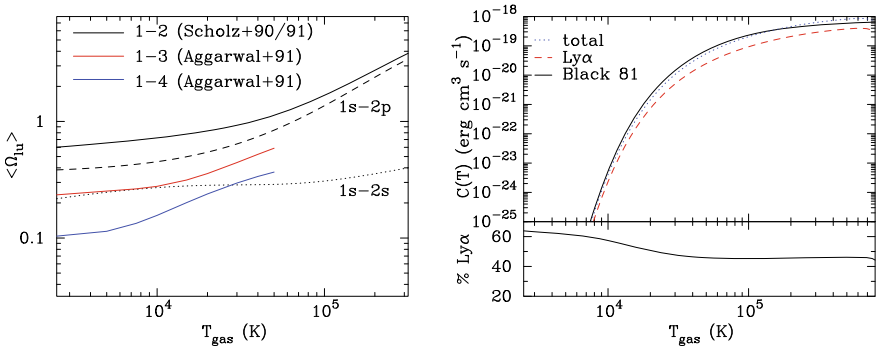

Fig. 1.7 *Left*: Velocity averaged collision strengths $\langle \Omega_{lu} \rangle$ are plotted as a function of temperature for the transitions $1s \rightarrow 2s$ (*dotted line*), $1s \rightarrow 2p$ (*dashed line*), and for their sum $1s \rightarrow 2$ (*black solid line*) as given by [236, 237]. Also shown are velocity averaged collision strengths for the $1s \rightarrow 3$ (*red solid line*, obtained by summing over all transitions $3s, 3p$ and $3d$), and $1s \rightarrow 4$ (*blue solid line*, obtained by summing over all transitions $4s, 4p, 4d$ and $4f$) as given by [10]. Evaluating the collision strengths becomes increasingly difficult towards higher n (see text). *Right:* The *blue-dotted line* in the *top panel* shows the total cooling rate per H-nucleus that one obtaines by collisionally exciting H atoms into all states $n \leq 4$. For comparison, the *red dashed* line shows the total cooling rate as a result of collisional excitation of the 2p state, which is followed by a downward transition through emission of a Lyα photon. All cooling rates increase rapidly around $T \sim 10^4$ K. The *lower panel* shows the ratio (in%) of these two cooling rates. This plot shows that ∼60% of the total gas cooling rate is in the form of Lyα photons at $T \sim 10^4$ K, and that this ratio decreases to ∼45–50% towards higher gas temperatures. At the gas temperatures at which cooling via line excitation is important, $T \lesssim 10^5$ K (see text), ∼45–60% of this cooling emerges as Lyα photons. Also shown for comparison as the *black solid line* is the often used fitting formula of [28], and modified following [47]

$$\frac{dE_{\rm th}}{dVdt} = n_e n_{\rm H} C(T), \tag{1.8}$$

where

$$C(T) = \sum_u q_{1s\rightarrow u} \Delta E_{1s\rightarrow u} \text{ erg cm}^3 \text{ s}^{-1}. \tag{1.9}$$

Here, the sum is over all excited states 'u'. The *blue-dotted line* in the *top right panel* of Fig. 1.7 shows $C(T)$ including collisional excitation into all states $n \leq 4$. The cooling rate rises by orders of magnitude around $T \sim 10^4$ K, and reflects the strong temperature-dependence of the number density of electrons that are moving fast enough to excite the hydrogen atom. For comparison, the *red dashed* line shows the contribution to $C(T)$ from only collisional excitation into the 2p state, which is followed by a downward transition through emission of a Lyα photon. The *lower panel* shows the ratio (in%) of these two rates. This plot shows that ∼60% of the total gas cooling rate is in the form of Lyα photons at $T \sim 10^4$ K, and that this ratio decreases to ∼45–50% towards higher gas temperatures. The *black solid line* is an often-used analytic fitting formula by [28]